Vol: 2, Pg: 16-25, Yr: 2021-AJABTR

Myogenic Tissue Regeneration: A New Insight

Biswadeep Chaudhuri

University of Engineering & Management, Newtown Kolkata

Corresponding: chaudhuri.biswadeep@gmail.com

Abstract:

Till today, the conventional therapeutic techniques are used to cure many muscle tissue related diseases. With the advent of modern science and technology, Tissue Engineering (TE) has evolved as a novel means to repair and regenerate different tissues. Recently graphene and graphene based composites are emerging as better materials compared to the conventional biopolymers to fabricate scaffolds for skeletal muscle TE and other biomedical applications. Addition of graphene oxide (GO) nanoplatelets (GOnPs) in bioactive polymers was found to enhance enhanced conductivity (σ) as well as dielectric permittivity (ε) of the scaffolds, due to the presence of GO surface charge, which enhance biocompatibility of the scaffolds. In the thesis work, for the first time, human Umbilical Cord Blood (UBC) derived mesenchymal stem cells (CB-hMSCs) were reported to directly differentiate to skeletal muscle cells (hSkMCs) on spin coated thin GO sheets, composed of GOnPs, and on electrospun fibrous meshes of GO–polymer (poly-caprolactone, PCL and poly lactic co-glycolic acid, PLGA)) composite meshes. These substrates exhibited excellent myoblast differentiations and promoted self-aligned myotubes formation similar to natural orientation. Scanning and transmission electron microscopy, Raman, infrared (vibration spectroscopic) etc. studies were carried out for the characterizations of GO sheet and the composite scaffolds. Significantly enhanced values of both conductivity and dielectric constant of the GO–Polymer composites attributed to the GO surface charge which provided favorable cues for the formation of superior cellular interaction and formation of multinucleated myotubes on the electrospun meshes. The present results demonstrated that such novel GO based polymer composite substrates might be used as potential candidates for the myoblast differentiation and proliferation of CB-hMSCs for the next generation skeletal muscle tissue repair and regeneration.

Introduction:

One of the current trends in tissue engineering (TE) is to fabricate excellent biocompatible substrates, which should offer appropriate guiding cues for the growth and proliferation of specific tissue types. Materials for such scaffolds should have suitable mechanical properties, chemical and biological compatibility and degrade in an appropriate time window. During the last couple of decades many electrospun nanofibrous scaffolds and carbon based nanomaterials (e.g. carbon nanotubes, nanodiamonds or graphene) have been widely investigated for different clinical and TE applications [1-3]. Recently, graphene and its derivatives have drawn special attention as novel nanomaterials with great potential in applications and utilizations such as photonics and optoelectronics, sensors, biomedical as well as TE, because of their extraordinary physicochemical properties and favourable bioactivity [2-6]. These properties further extended their intensive applications for the differentiation of human neural stem cells, osteogenic differentiation of human stem cells, drug delivery and also in photothermal cancer therapy. An injectable graphene/hydrogel-based gene delivery system has been developed for vasculogenesis and cardiac tissue repair [5-7]. The antibacterial property, anti-inflammatory effects and biocompatibility of graphene and graphene oxide nanoplatelets (GOnPs) were also tested

with mammalian cells by different research groups. We used GOnPs sheet and GOnPs – polymer composite electrospun meshes for the myoblast differentiation of human cord blood stem cells. We also tried to find the origin of the excellent biocompatibility of GO and GO polymer composites based on GO surface change which enhanced the conductivity of the composite meshes.

It is a constant effort for the researchers to find most suitable materials for biomedical applications. Till now there are various conducting scaffolds have been developed for skeletal muscle tissue engineering applications. But there is need for further development. Various physicochemical as well as biological properties of GO have already been discovered [1-6]. Low conducting high dielectric GO possesses surface charge and also PE properties which are also stimulants for cells growth. Conductivity ,dielectric constant and piezoelectric properties are associated with surface charge (PE coefficient d33 is related to dielectric constant) of oxides and polymers scaffold materials. PE and dielectric properties are the unique universal properties of living tissues, and may play a significant role in several physiological phenomena. Therefore, σ, ε, Q and PE properties, which vary with GO concentration might appear to be relevant for the biocompatibility of graphene based materials for different biomedical and tissue regeneration applications [8-12]. A few detailed studies on the relationship between human stem cell and graphene have drawn a tremendous impetus in the field of different TE applications [12-18]. These investigations were carried out mainly with bone marrow derived mesenchymal stem cells, iPSCs and neural cells [19-26]. Although mouse myoblast proliferation on rGO deposited modified glass substrate was reported, no study focussed on the proliferation and differentiation of human mesenchymal stem cells to skeletal muscle cells on GO sheet or GO–polymer fibrous scaffold. Present studies are important for exploring the possibility of fabricating different GO– polymer based biocompatible conducting electrospun scaffolds for myoblast differentiation human stem cells for the repair and regeneration of skeletal muscle and other tissues.

Preparation of GO sheet and GO–Polymer meshes

GOnPs were synthesized from graphite powder similarly to our previous work following the modified Hummers method. In brief, graphite (2 g), sodium nitrate (1 g) and H2SO4 were added to a 250 ml flask kept at 0 °C. Concentrated H2SO4 (50 mL) was then poured slowly while stirring keeping temperature below 5 °C. The mixture was then stirred for 30 min and 0.3 g of KMnO4 powder was added while the system was maintained at 35°C for 30min. The mixture was further diluted with warm water and treated with H_2O_2 to remove residual KMnO4 until bubbling disappeared. The resulting solution was centrifuged at 6500 rpm for 45 min for three times and 1N NaOH was added to adjust the pH value of the solution to 7.4 approximately. The solid mass thus synthesized was washed with de-ionized water to obtain pure GOnPs used to make thin GO sheet by spin coating and GO–PCL meshes by electrospinning techniques. Spin coated thin GO sheets (20–60 μm thickness depending on GO concentration in DMF) on cleaned glass plates and Teflon sheets were prepared fromDMF solutions of GOnPs by sonicating the mixture for 2h. to uniformly disperse GO nanoparticles. The dried thin GO sheets were peeled off the glass/Teflon substrates which were used for cell culture after vacuum drying at around 37 °C for about 3 h. Electrospun fibrous meshes were prepared from the GO–PCL–DMF solution. To make composite solution, PCL (1 g in 25ml DMF solution) and GO (20 μgml−1 PCL/DMF solution) were mixed and sonicated for 45–50min. The final colloidal solution loaded into a 10mL plastic syringe with a stainless ssteel needle (diameter ∼0.65 mm)

was used for making electrospun scaffolds using electrospinning (PICO ESPIN, India).

Physicochemical characterization of GO sheet and GO–PCL meshes

Thin GO sheet and GO–PCL composite meshes were characterized by x-ray diffraction (XRD) (Philips Shiffert 3710 diffractometer using Cu–Kα radiation source) analysis, scanning electron microscopy (SEM: JEOL JSM 6400), field emission scanning electron microscope (FESEM:Model JEM-2012, JEOL) and high resolution transmission electron microspore (HRTEM: Model JEM-2010, JEOL) studies. Raman spectroscopy (HORIBA JOBIN Yuon: exciting wavelength 514 nm with argon ion laser), ultraviolet and visible (UV) (300–800nm) and Fourier transform infrared (FTIR: Perkin–Elmer spectrum 100 FTIR spectrometer with a 4 cm−1 resolution) spectroscopic studies were also carried out for characterizing GO and GO–PCL composite. Water contact angle (CA) measurements against distilled water were performed using a sessile drop method (DAS100S: KRUSS GMbH, Germany). The advancing (wetting CAw) and receding (dewetting CAdw) CAs were measured at RT at different locations for the GO sheets. Mechanical characterization of the GO sheet was performed by uniaxial tensile testing. GO sheets were carefully cut into rectangular stripes (15×30mm) and loaded with an Instron 3369 tensile strength measuring system. A segment of electrospun meshes (10 × 25 mm) was fixed at the cut ends for the axial testing (n = 5). Frequency dependent conductivity and dielectric constant (ε) of the GO sheet and electrospun meshes were measured using impedance analyser (HP Model 4194A) similarly to our previous work. For electrical measurements electrodes on the surfaces of the samples were made by high quality silver paint which was dried in vacuum. To estimate in vitro stability and biodegradation of the GO sheets, we also studied σ and ε values of GO sheet and composite meshes after immersion in PBS solution for 7 days at ambient temperature. After immersion, both the samples were removed from the soaked solution washed with deionised water, and dried in a vacuum chamber to remove moisture, before electrical measurements.

Cell seeding, myoblast differentiation and myotubes formation

The mesenchymal stem cells, CB-hMSCs, used for differentiation to skeletal muscle cells on the GO sheet and GO–PCL mesh were isolated from human UCB similarly to previous method [69, 73]. UCB was collected from ISPAT General Hospital, Rourkela with patient's consent. All procedures were approved by the National Institutional Ethical Committee.

UCB derived CB-hMSCs (5×10^3 cells/well) were directly seeded on the thin film likeGO sheet (~30 μm thick) and GO–PCL mesh (areas ~45mm2) as well as on electrospun collagen fibrous meshes and collagen coated glass as controls(hereafter referred to as controls) in a 12 well plate and cultured with skeletal muscle differentiation media (90v/v%) supplemented with FBS (10v/v%) and 100x antibiotic–antimycotic solution (1v/v% approximately), and incubated at 37°C and 5%CO2 atmospheric condition. In addition, insulin like IGF-1 was added (5ng ml−1) to enhance the myogenic differentiation process. After 12–15 days of culture, cells morphology was found to change towards bipolar skeletal myoblasts (hSkMCs). Low serum (2% horse serum) media was introduced to enhance myoblast

Immunostaining Analysis

For immunostaining analysis, hSkMCs grown after 5 days of culture on different substrates (i.e. collagen and glass controls, GO sheets and GO–PCL/PLGA meshes) were analysed for the expression of myogenin, an early myogenic differentiation marker. Briefly, to detect myogenin, cells werefixed and incubated with primary antibody (1:100) at 4 °C overnight and after washed with PBS, again incubated with secondary antibody DyLight

488-conjugated goat anti-mouse IgG (1:100) at RT for 1 h. before viewing. On 11 days of culture, cells were analysed for further expression of muscle specific antigens such as myosin heavy chain (MHC) and dystrophin. Cells were fixed with 4% paraformaldehyde, permeabilized with 0.1% Triton X-100, and then incubated in goat polyclonal anti-MHC (1:100) and rabbit polyclonal anti-dystrophin (1:100) as primary antibodies for 1 h. Next, after washing with PBS, a FITC conjugate rabbit anti-goat secondary antibody (1:500) was used to detect MHC, while Texas Red conjugated goat anti-rabbit secondary antibody (1:150) was also employed to detect dystrophin. The samples stained without primary antibody served as negative controls. Nuclei were counterstained with 4′,6-diamidino-2-phenylindole (DAPI).

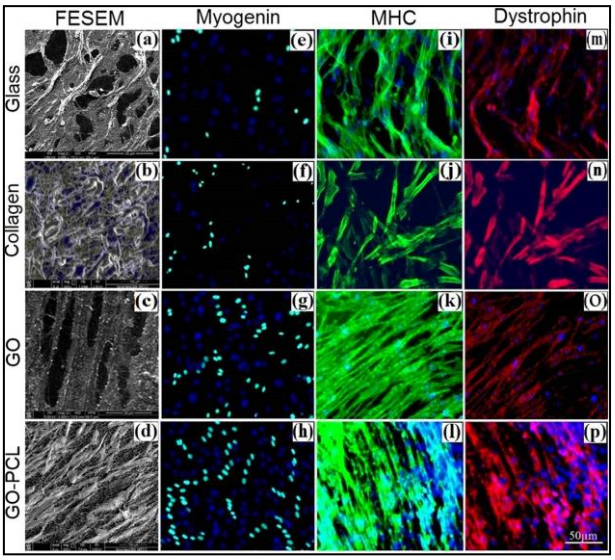

Figure 1: FESEM micrographs showing formation of myotubes on samples (a-d). Immunostaining analysis of Myogenin, MHC and Desmin on specific samples after 7 days of culture. Nuclei were counterstained with DAPI. (Chaudhuri et.al. Biofabrication 2015)

Fluorescence-activated cell sorter (FACS) analysis

The skeletal muscle cells adhered onto the GO sheet, GO–PCL meshes and controls were trypsinized and FACS analysis was performed to verify the expression of skeletal muscle differentiation markers like CD56 and desmin. For all antibodies, 5 × 105 cells were incubated in 100 ml of PBS containing 1%FBS and the dilution of primary antibodies ranged from 1:15 to 1:100. The cells after being incubated with primary antibody on ice for 30 min, were washed with 1% FBS in PBS, re-suspended in 100 ml of FITC-labelled secondary antibody, diluted 1:100 in 1% FBS in PBS and incubated again for 30 min on ice. Finally, the cells were washed with PBS containing 1% FBS prior to resuspension in PBS with 1% FBS for FACS analysis. Isotype-matching immunoglobulin (IgG) and FITClabelled secondary antibody were used to determine nonspecific signals. FACS analyses were performed with a BD LSR Fortessa (San Jose, CA, USA) equipped with an air cooled argon laser. FACS data were analysed by FCS Express software.

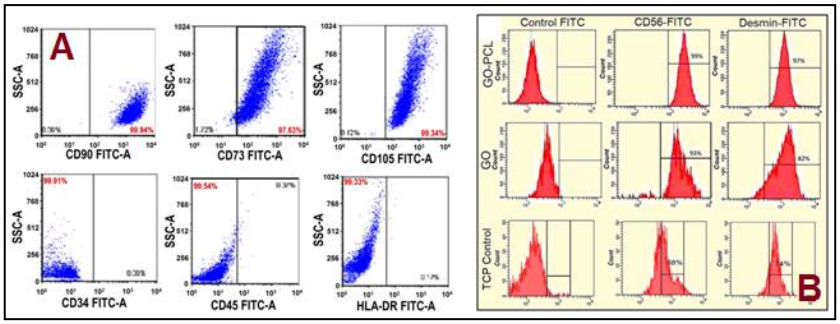

Figure 2: FACS analysis of (A) UCB derived MSCs with positive & negative markers. (B) Muscle specific markers CD56 and Desmin. FACS analysis indicated differentiation of CB-MSCs to skeletal muscle cells. .(Chaudhuri et.al. Biofabrication 2015).

Cells adhesion from FESEM analysis

Cells adhesion on the different substrates was studied by SEM/FESEM analysis. After 11 days of culture, the cells seeded on all the substrates were carefully washed twice with PBS, fixed with 2.5% glutaraldehyde for 4 h and then dehydrated through a gradient series of ethanol from 70 to 100%. All the said substrates were then carefully dried using a vacuum desiccator to make them moisture free prior to FESEM analysis.

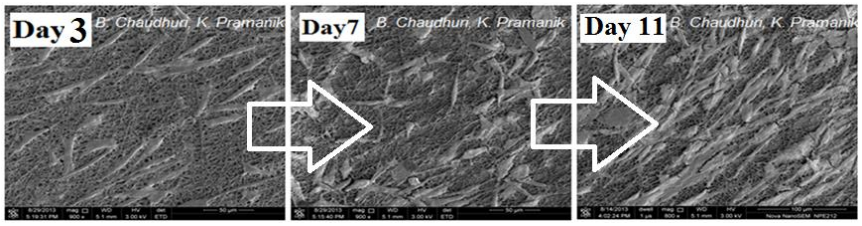

Figure 3: FESEM micrographs indicating cells adhesion on (GO-PCL) composite scaffolds and also gradual proliferation from day 3 to 11. .(Chaudhuri et.al. Biofabrication 2015).

Cell morphology and Aspect Ratio

The morphology of skeletal muscle cells were analysed using cytoskeleton staining after 3 days of culture. Cells were fixed with 4% paraformaldehyde, permeabilized with 0.1% Triton X-100 and stained with FITC-phalloidin. Nuclei were counterstained with DAPI. The actin filaments and nuclei were observed using a Zeiss Axivert 40 CFL fluorescence microscope. Cell morphology was much elongated and aspect ratio was much higher on GO based substrates indicating better myoblast differentiation potential.

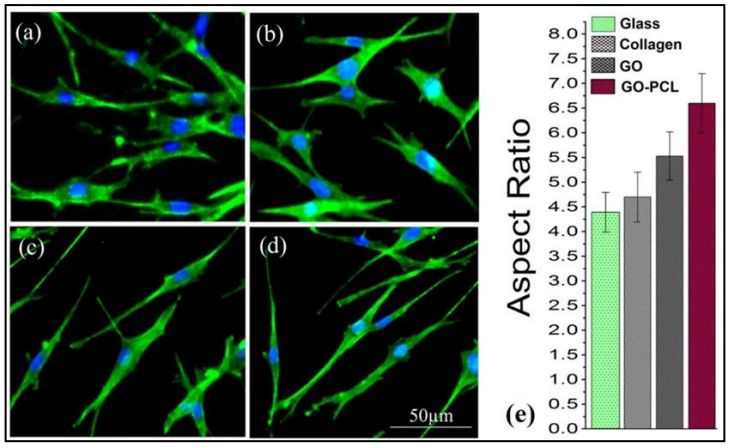

Figure 4: Cell morphological analysis (a-d) showing more elongated SkMCs on GO (c, d) based substrates compare to controls (a,b). (e) Represents Quantitative analysis of cell aspect ratio. .(Chaudhuri et.al. Biofabrication 2015).

Cell viability and proliferation

Cell viability and proliferation on GO/PCL composite meshes, thin GO sheet and controls were measured by water-soluble tetrazolium salt (WST-8) assay after 3, 7 and 11 days of cell seeding in 12 well culture plate. Ten µl of cell proliferation reagent (WST-8) was added into each well containing sample with 100 µl of culture medium and incubated for 4 h at 37 °C. Absorbance (OD) of the solution was then measured at 450 nm by a microplate reader(Varioskan Flash, Thermo Scientific). The cells seeded on collagen scaffolds were evaluated as control. WST- 8 was reduced by dehydrogenase activities of living cells that give rise yellow-colour formazan dye. The amount of formazan dye generated (by the activities of dehydrogenases) was directly proportional to the number of living cells.

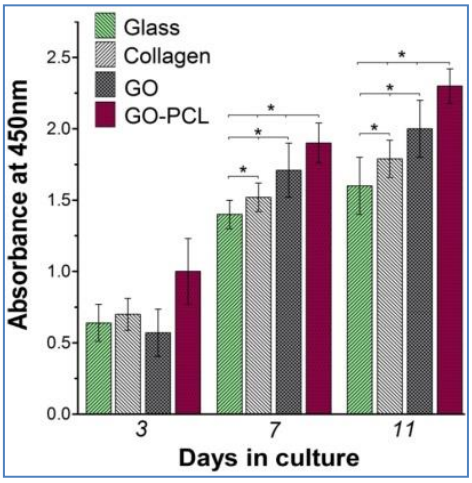

Figure 5: Cell viability and proliferation assay (via WST-8 assay). Results presents as mean ± SD. * indicates significant difference (n=5, $p<0.05$). .(Chaudhuri et.al. Biofabrication 2015).

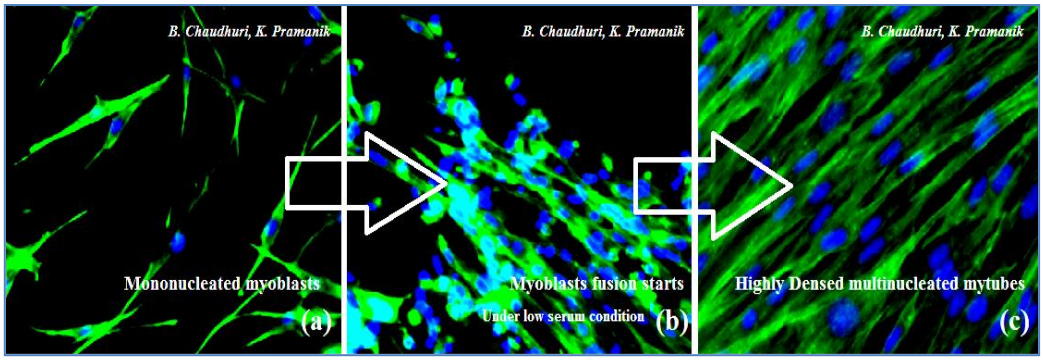

Figure 6: Gradual Cells proliferation (day 3(a), 7(b), 11(c)) indicating biocompatibility of GO-PCL composite scaffolds (a-c) .(Chaudhuri et.al. Biofabrication 2015).

Conductivity (σ), dielectric constant (ε) and in vitro stability of thin GO sheet and GO–PCL meshes and origin of enhanced biocompatibility of GO based materials

Figures 7 showed an increase of both ε (~300 for GO–PCL and only 25 for PCL) and σ (more than two orders of magnitude higher in GO–PCL compared to that of PCL) for GO–PCL meshes, which was due to the presence of GO in PCL. Similar enhancement of σ and ε was also observed in GO–PVA and other GO–polymer composites. Enhancement of σ and ε in GO–PCL might be due to the formation of conducting pathways betweenthe more conducting deformed GOnPs sheets (enhancing σ) and the creation of micro-capacitors with insulating PCL acting as dielectric films. In GO sheets, a mixture of both positive and negative charges is present, which lead to a decrease of σ, but to an increases in polarizability (PE) and hence dielectric constant. It is further noticed that both σ and ε values of GO sheets and GO–PCL meshes slightly decreased with increasing of immersion time in PBS indicating in vitro stability. Moreover, no significant morphological change of the GO sheets was observed as indicated by FESEM (Fig. 7e). The addition of GO also reduced the degradation rate of GO–PCL (compared to PCL only), as revealed from the lower decreasing rates of σ and ε compared to those of PCL. Therefore, this study highlighted that both GO sheets and GO–PCL meshes could retain their σ and ε and hence stability over one week. The controllable enzymatic degradation of graphene/PCL materials was studied and these substrates were proved to be promising biodegradable electro-responsive scaffolds for skeletal muscle TE applications. Even the degradation products of the composite materials were reported to exhibit less inhibition to cell metabolism and proliferation than the degradation products of pure PCL. Controllable non-toxic degradation and unique physical properties confirmed that covalently-linked PCL–graphene based composites are ideal materials for the development of electro-responsive scaffold for muscle TE.

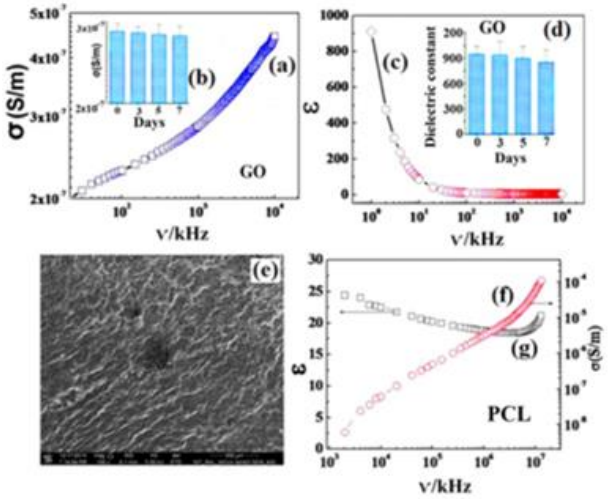

Figure 7. Conductivity and dielectric stability of thin GO sheet and GO-polymer composite (a-d). SEM micrograph of GO sheet after immersion in BSF for seven days and (f,g) Change of conductivity and dielectric constant after immersion for seven days. .(Chaudhuri et.al. Biofabrication 2015).

Physicochemical Characterizations

Physicochemical Characterizations of scaffolds via XRD, FTIR, Raman Spectra analysis indicates presence of GO and PCL in our composite scaffolds.

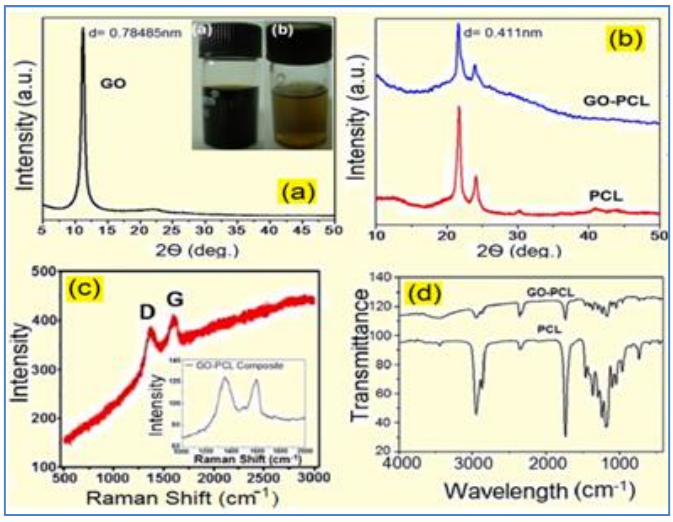

Figure 8. XRD of GO, GO-PCL and PCL (a, b). Raman spectra of GO and GO-PCL (c). FTIR analysis of GO-PCL and PCL (d). .(Chaudhuri et.al. Biofabrication 2015).

Contact angle and mechanical property of GO sheet and GO-PCL meshes

Wetting (CA_w) and dewetting (CA_{dw}) contact angles of thin GO sheet and GO-PCL mesh films are shown in fig. 9. In case of thin GO sheets, CA_w was found to be around ~58.7° with hysteresis (CA_w-CA_{dw}) of ~4° which might be a measure of the solid-liquid interaction. For the GO-PCL meshes, the contact angle (CA) was ~75°. Due to the presence of GO with abundant hydroxyl group, CA of GO-PCL significantly ($p<0.05$) decreased compared to PCL, (CA ~119°). It is suggested that GO-PCL composite fibrous meshes could enhance cell adhesion as they are more hydrophilic and have higher surface energy due to the presence of GO. The stress-strain curves of GO sheets and GO-PCL meshes were shown in figure 4.11b. The

tensile strength of PCL (~1.8MPa) was found to increase significantly with addition of GO (~4.0MPa). The tensile strength is also known to increase with increasing GO concentration. Favourable contact angle and mechanical properties supported GO and GO-PCL meshes for tissue engineering applications.

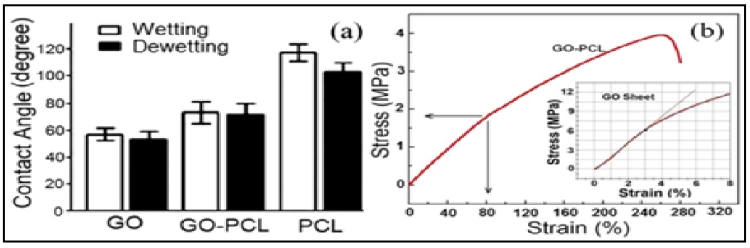

Figure 9. (a) contact angle showing advancing (wetting) and receding (dewetting) water sessile drop on GO sheet, GO-PCL and PCL meshes. (b) stress-strain curves of GO-PCL meshes and thin sheet. .(Chaudhuri et.al. Biofabrication 2015).

Conclusion

In this thesis work, we demonstrated, for the first time, that antibacterial and anti-inflammatory thin GO a sheet and GO–PCL and PLGA-GO nanofibrous meshes (within non-toxicity limit) are excellent biocompatible substrates for hSkMCs differentiation of cost effective cord blood stem cells CB-hMSCs. Similar trend was also found in case of IGF-1 pathway (that was assessed later on) that too was enhanced by addition of GOnPs in polymer. The specific physicochemical properties (like adsorption of small molecules on GO surface, graphene with many oxygen-containing functional groups, such as hydroxyl, carboxyl and epoxy groups) offered by GO-based polymer biomaterials favored cells growth and proliferation. Myoblast differentiation capability of thin GO sheet and its polymer composites meshes were attributed to its surface change, and nano-structured surface morphology. Addition of GOnPs enhanced both conductivity and dielectric constant (related to surface charge) of these composite scaffolds and provided supporting cues stimulating highly oriented multinucleated myotubes formation, similar to natural orientation, which is highly desirable for the regeneration of functional skeletal muscle. In demand of cell specific substrates for the next generation of TE applications, the use of GO sheets and GO-based polymer composite meshes in combination with easily available CB-hMSCs might be considered as most favourable candidates for future skeletal muscle regenerations.

References:

[1] Bach AD, Beier J P, Staeter J and Horch R E 2004 Skeletal muscle tissue engineering J. Cell Mol. Med. 4 13–22

[2] ChenGP, Ushida T and Tateishi T 2002 Scaffold design for tissue engineering Macromol. Biosci. 2 67–77

[3] SabirML,XuXand Li I 2009 A review of biodegradable polymeric materials for bone tissue engineering applications J. Mater. Sci. 44 5713–24

[4] Yan X, Chen J, Yang J, XueQandMiele P 2010 Fabrication of free-standing, electrochemically active, and biocompatible graphene oxide–polyaniline and graphene–polyaniline hybrid papers ACS Appl. Mater. Interfaces 9 2521–9

[5] Baker SC, Rohman G, Southgate J and CameronNR 2009 The relationship between the mechanical properties and cell behavior of PLGA and PCL scaffolds for blended tissue engineering Biomaterials 30 1321–6

[6] WanCand Chen B 2011 Poly(ε-caprolactone)/graphene oxide biocomposites: mechanical properties and bioactivity Biomed. Mater. 6 055010–8

[7] Ravichandran R, Sundarrahjan S, Venugopal R J, Mukherjee S and Ramakrishna

S 2010 Application of conducting polymers and their issues in biomedical engineering J. R. Soc. Interface 7 S559–79
[8] ChenMC, Sun YCand Chen YH2013 Electrically conductive nanofibers with highly oriented structures and their potential application in skeletal muscle tissue engineering ActaBiomaterialia 9 5562–72
[9] Kim H, AbdalaAAandMacosko CW2010 Graphene/ polymer nanocomposites Macromolecules 43 6515–30
[10] Markovic ZM, Harhaji-Trajkovic LM, Todorovic-Markovic BM, KepićDP, ArsikinKM, Jovanović S P, PantovicAC, DramićaninMDandTrajkovicVS 2011 In vitro comparison of the photothermal anticancer activity of graphene nanoparticles and carbon nanotubes Biomaterials 32 1121–9
[11] Choi J S, Lee S J, ChristGJ, AtalaAandYoo J J 2008 Influence of electrospun aligned poly (e-caprolactone)/collagennanofiber meshes on the formation of self-aligned skeletal muscle myotubes Biomaterials 29 2899–906
[12] Sebaa M, Nguyen T Y, Paul RK, Mulchandani A and LiuH 2013 Graphene and carbon nanotube–graphene hybrid nanomaterials for human embryonic stem cell culture Mater. Lett. 92 122–5
[13] Kolbacova M, Broz A, Kong J and KalbacM2010 Graphene substrates promote adherence of human osteoblasts and mesenchymal stomalcells Carbon 48 4323–9
[14] HuH, Ni Y, Montana V, Haddon RCand ParpuraV2004 Chemically functionalized carbon nanotubes as substrates for neuronal growth Nano Lett. 4 507–11
[15] Malarkey E B, Fisher AK, Bekyarova E, Liu W, Haddon RCand ParpuraV2009 Conductive single walled carbon nanotubes modulate neural growth Nano Lett. 9 264–8
[16] Wang K, Ruan J, Song H, Zhang J and CuiD2011 Biocompatibility of graphene oxide Nanoscale Res. Lett. 6 8
[17] Bonaccorsa F, Sun Z, Hasan T and Ferrari AC2010 Graphene photonics and optoelectronics Nat. Photonics 4 611–22
[18] Liu Y, Yu D, Zhang C, Miao Z and Dai L 2010 Biocompatible graphene oxide based glucose biosensor Langmuir 26 6158–60
[19] Sanigrahi J, BhadraDand Chaudhuri BK2012 Crystalline graphite oxide/PVDF nanocomposite gate dielectric: lowvoltage and high field effect mobility thin-film transistor Phys. Status Solidi 210 546–52
[20] Gaharwar AK, PeppasNAandKhademhosseini A 2014 Nanocomposite hydrogels for biomedical applications Biotechnol. Bioeng. 111 441–53
[21] Ryu S and Kim B S 2013 Culture of neural cells and stem cells on graphene Tissue Eng. Regenerative Med. 10 39–46
[22] Ku SHandParkCB 1913 Myoblast differentiation on graphene oxide Biomaterials 34 2017–23
[23] AkhavanOandGhaderi E 2013 Graphene nanomesh promises extremely efficient in vivo photothermal therapy Small 9 3593–601
[24] Akhavan O, Ghaderi E and ShahsavarM2013 Graphene nanogrids for selective and fast osteogenic differentiation of human mesenchymal stem cells Carbon 59 200–2211 [25] Zhang LM, Xia JG, ZhaoQH, Liu LWand Zhang Z J 2010 Functional graphene oxide as a nanocarrior for controlling loading and targeted delivery of mixed anticancer drugs Small 6 537–44
[25] ChenGY, PangDW, Hwang SM, TuanHY and HuYC 2012 A graphene-based platform for induced pluripotent stem cells culture and differentiation Biomaterials 33 418–27
[26] Lee CS et. al. TRIM72 negatively regulates myogenesis via targeting insulin receptor substrate-1. Cell Death and Differentiation (Nature Publishing Group). 17, 1254–1265. 2010.